LETTERS

Emergence of preformed Cooper pairs from the doped Mott insulating state in $Bi_2Sr_2CaCu_2O_{8+\delta}$

H.-B. Yang[1], J. D. Rameau[1], P. D. Johnson[1], T. Valla[1], A. Tsvelik[1] & G. D. Gu[1]

Superconductors are characterized by an energy gap that represents the energy needed to break the pairs of electrons (Cooper pairs) apart. At temperatures considerably above those associated with superconductivity, the high-transition-temperature copper oxides have an additional 'pseudogap'. It has been unclear whether this represents preformed pairs of electrons that have not achieved the coherence necessary for superconductivity, or whether it reflects some alternative ground state that competes with superconductivity[1]. Paired electrons should display particle–hole symmetry with respect to the Fermi level (the energy of the highest occupied level in the electronic system), but competing states[2–4] need not show such symmetry. Here we report a photoemission study of the underdoped copper oxide $Bi_2Sr_2CaCu_2O_{8+\delta}$ that shows the opening of a symmetric gap only in the anti-nodal region, contrary to the expectation that pairing would take place in the nodal region. It is therefore evident that the pseudogap does reflect the formation of preformed pairs of electrons and that the pairing occurs only in well-defined directions of the underlying lattice.

Angle-resolved photoemission spectroscopy (ARPES; see Supplementary Information) has been used extensively to study the copper oxide superconductors[5–8]. It has been concluded that in the superconducting state, the energy gap associated with the electron pair has *d*-wave symmetry with maximum gap in the anti-nodal region, and that in the normal state a pseudogap, also in the same region, coexists with 'Fermi arcs'. These arcs extend out from the nodes (points where the superconducting gap has zero value) with a length proportional to T/T^*, T^* being the pseudogap onset temperature[9]. It is generally assumed that the spectral function, the response to the addition or removal of an electron, is particle–hole symmetric around the Fermi surface at low energies, with a peak at the Fermi level on the Fermi arcs and a local minimum at the Fermi level in the gapped regions away from the arcs[10]. In Bardeen–Cooper–Schrieffer theory, the superconducting gap reflects the formation of electron pairs in parallel with the development of long-range phase coherence. The spectral function associated with the paired electrons will consist of two peaks displaying particle–hole symmetry with respect to the Fermi level (see Supplementary Information).

Several techniques have been used in ARPES to obtain a more representative picture of the complete gap. These include 'symmetrization' of the measured photoemission intensity to produce an identical spectral response in both the occupied and the unoccupied states[11]. A second method uses the fact that the measured photoelectron intensity as a function of energy ω and momentum $\mathbf{k}$, $I(\mathbf{k},\omega)$, is given by

$$I(\mathbf{k},\omega) \propto \int A(\mathbf{k},\omega')f(\omega')R(\omega-\omega')\,\mathrm{d}\omega' \qquad (1)$$

with $A(\mathbf{k},\omega)$ the spectral function, $f(\omega)$ the Fermi distribution function and $R(\omega)$ the experimental resolution. The proportionality indicates the presence of a matrix element dependent on the photon energy. Some level of information can thus be obtained on states thermally occupied above the Fermi level, by dividing the measured intensity by the appropriate temperature-dependent Fermi function. The procedure enhances the response above the chemical potential, but is complicated by the fact that the measured spectral intensity also reflects the experimental resolution. In the past, either the role of the experimental resolution has been ignored or the raw data have been normalized to a Fermi function convoluted with a representative resolution function[11–14].

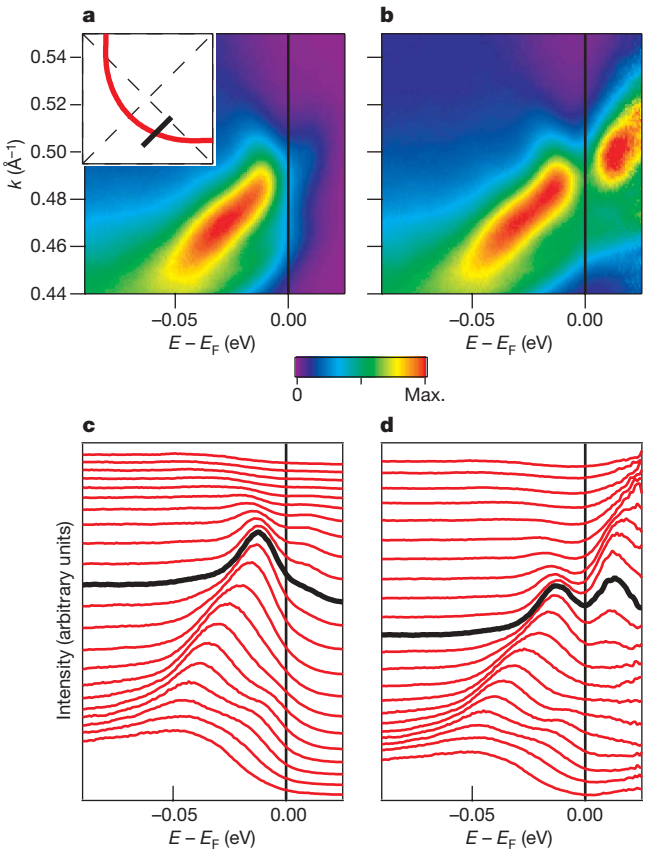

Figure 1 | Analysis of spectra from the optimally doped material. Spectral plots of optimally doped ($T_c = 91$ K) BSCCO as recorded (**a**) and after the analysis described in the text (**b**). The spectra were recorded at a temperature of 80 K and at the point in the Brillouin zone indicated in the schematic in the inset of **a**, where the red line indicates the Fermi surface. The incident photon energy was 16.5 eV. **c**, **d**, EDC cuts through the spectral plots of **a** and **b**, respectively. The EDCs corresponding to $\mathbf{k}_F$ are indicated. The spectra in **d** show the dispersion of the Bogoliubov quasi-particles in complete agreement with equation (1).

[1]Condensed Matter Physics and Materials Science Department, Brookhaven National Laboratory, Upton, New York 11973, USA.

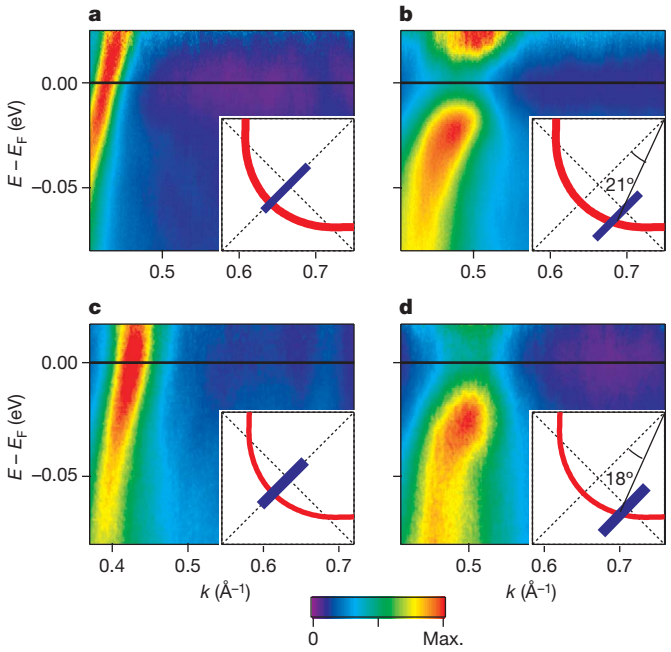

Figure 2 | Spectra from the optimally doped and underdoped material in the superconducting state. Spectral plots after the full analysis as discussed in the text for optimally doped ($T_c = 91$ K) and underdoped ($T_c = 65$ K) BSCCO in the superconducting state. The incident photon energy was 16.5 eV. **a**, **b**, Spectral plots recorded from the optimally doped sample at a temperature of 80 K in the nodal direction (**a**) and away from the nodal direction (**b**) as indicated in the Brillouin zones shown in the respective insets. **c**, **d**, Same as **a** and **b**, but for the underdoped material at a temperature of 50 K, again as indicated in the insets. **b** and **d** show the presence of a symmetric superconducting gap.

These methods can lead to serious errors in the relative intensity above and below the Fermi energy, E_F, and to distortions of band dispersions in the vicinity of the Fermi level.

We develop two different approaches to circumvent these problems. The two methods give nearly identical results for the purposes of this study. The first amounts to an approximate solution of equation (1). A function $S(\mathbf{k}, \omega) = A(\mathbf{k}, \omega)f(\omega)$ is determined by convolving $I(\mathbf{k}, \omega)$ with a function that is effectively the inverse transform of a momentum-independent resolution function $R(\omega)$, the latter assumed to be of Gaussian form (see Supplementary Information). Dividing the obtained $S(\mathbf{k}, \omega)$ by the Fermi distribution function, $f(\omega)$, then provides access to the states above the Fermi level.

The second method (see Supplementary Information) uses the fact that the two-dimensional energy-momentum information recorded in modern electron spectrometers is simply an image captured by an array of pixels. In an ideal world with infinite energy and momentum resolution, each pixel i would capture the relevant information, S_i. We use identical labelling in discussing the two methods, to make the discussion more transparent. Thus, S_i is equivalent to the component of the spectrum $S(\mathbf{k}, \omega)$ captured by pixel i. The finite resolution of the system results in the information S_i being distributed across neighbouring pixels with Gaussian widths defined by the experimental resolution. The energy and angular broadening are simultaneously removed using the so-called Lucy–Richardson iterative technique, which is a procedure frequently used in the analysis of medical and astronomical images[15] (see Supplementary Information).

Figure 1 shows the results of such an analysis applied to the spectral intensity measured from an optimally doped ($T_c = 91$ K) $Bi_2Sr_2CaCu_2O_{8+\delta}$ (BSCCO) sample in the superconducting state. The dispersion of the Bogoliubov quasi-particles above and below the Fermi level with the transfer of intensity from the occupied to unoccupied states at $\mathbf{k}_F$, the Fermi wavevector, is in complete accord with the Bardeen–Cooper–Schrieffer spectral function (see Supplementary Information).

Figure 2 compares the behaviour in the underdoped and optimally doped systems in the superconducting state. For both samples, the spectra show the opening of a symmetric gap on moving away from the node. Figure 3 shows similar spectra but now in the normal state, above T_c. The spectra from the optimally doped sample show

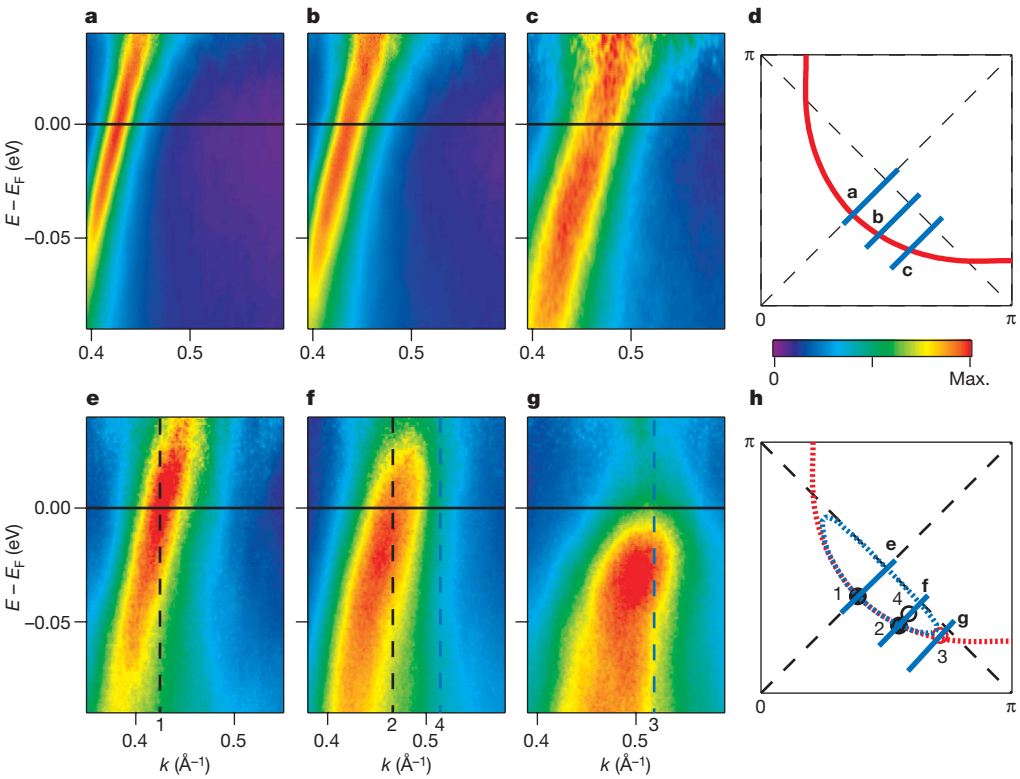

Figure 3 | Spectra from the optimally doped and underdoped material in the normal state. Spectral plots after the full analysis as discussed in the text for optimally doped ($T_c = 91$ K) and underdoped ($T_c = 65$ K) BSCCO in the normal state. The incident photon energy was 16.5 eV and in all cases the spectra were recorded at a temperature of 140 K. **a**, **b**, **c**, Plots recorded from the optimally doped material in the nodal direction and away from the nodal direction, as indicated in **d**. **e**, **f**, **g**, Same as **a**, **b** and **c**, but for the underdoped material, as indicated in **h**. The magnetic zone boundary would lie at $k = 0.58$ Å^{-1}. In **e** and **f**, the vertical black dashed line indicates the Fermi surface crossing. In **f** and **g**, the vertical blue dashed line indicates the turning point at the top of the dispersion. These are indicated in **h** by the open circles, black indicating a turning point above the Fermi level and red a turning point below the Fermi level. The filled black circles indicate the position of Fermi crossings. The possible pocket is indicated by the area enclosed by the blue dashed line in **h**.

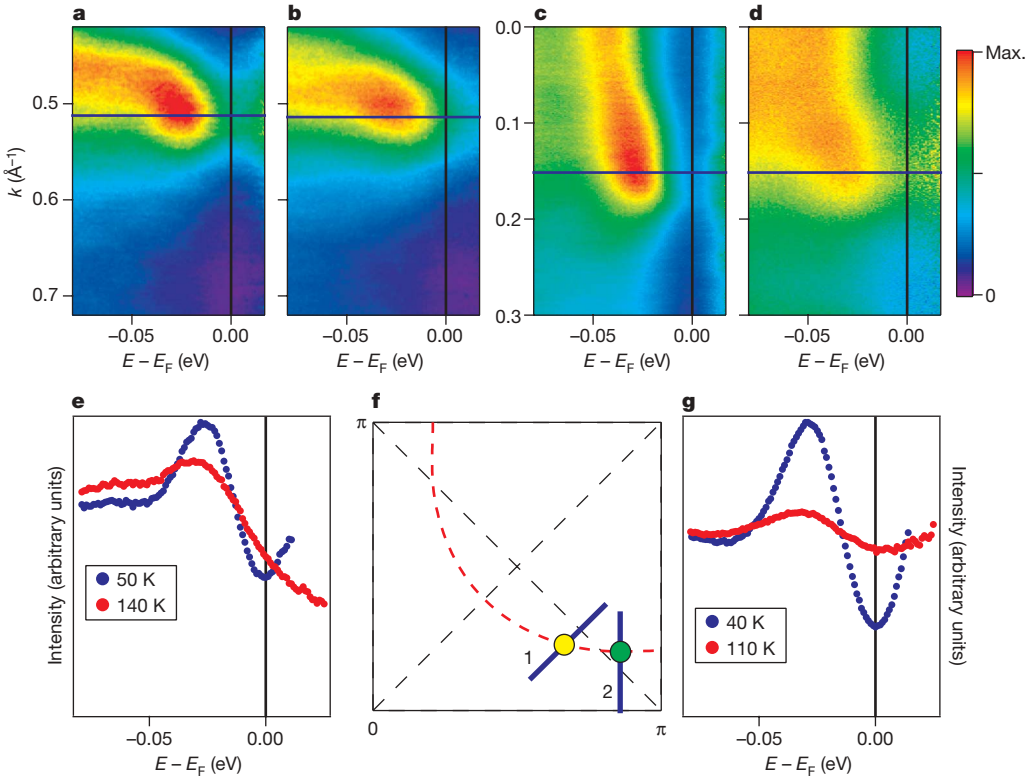

Figure 4 | Analysis of spectra recorded along the anti-nodal direction. Comparison of the spectral plots after analysis, and associated EDCs for two different regions of the Brillouin zone, both in the normal and superconducting states for the underdoped 65 K sample. These are shown in **a**, **b** and **e** for the region showing particle–hole asymmetry and in **c**, **d** and **g** for the region near the anti-node, as indicated in **f** (points 1 and 2, respectively). **a**, Spectral intensity recorded from point 1 at a temperature of 50 K; **b**, same as **a**, but in the normal state at a temperature of 140 K. **c**, Spectral plot from point 2 recorded at 40 K; **d**, same as **c**, but in the normal state at 110 K. **e**, EDCs cut through the plots associated with point 1 show particle–hole symmetry in the superconducting state and asymmetry in the normal state. **g**, EDCs cut through the plots associated with point 2 show particle–hole symmetry in both the superconducting and normal states.

the closing of the gap, as might be anticipated. However, in the normal-state spectra recorded from the underdoped material, the striking observation is the loss of particle–hole symmetry and the appearance of a gap above the chemical potential. In particular, it appears that on moving away from the node a gap appears in the spectrum and moves down to straddle E_F farther from the node. If the spectrum were symmetrized in energy at $k = |\mathbf{k}_F|$ in Fig. 3f, it would incorrectly indicate the presence of a particle–hole symmetric pseudogap.

The observation of a gap above E_F, together with the absence of particle–hole symmetry in the underdoped sample, suggests the absence of pairing in the nodal region in the normal state. There are several different theoretical explanations for the gap at positive energies. Some suggest a competing order associated with the underlying antiferromagnetism, with the gap reflecting the magnetic zone boundary[16,17]. Others suggest that the normal state represents a disordered spin liquid[18–20]. This in turn represents a particle with spin moving through a sea of spins (the Mott insulating state) rather than representing a Fermi liquid, where an electron or hole moves through a sea of electrons. In all of the models, the observed Fermi arc actually represents the inner half of a hole pocket, the outer half being suppressed by coherence factors, similar to the suppression of the Bogoliubov quasi-particles observed in Fig. 1. The two sides of the pocket are defined by bands dispersing up through the Fermi level, turning back at the gap edge and dispersing down through the Fermi level again. A representative pocket is indicated by the dashed blue line in Fig. 3h. The present experimental observations of a folding in the dispersion (representative energy distribution curves (EDCs) are shown in the Supplementary Information) followed by a loss of intensity is fully consistent with such a picture. However, we are able to make one other important observation based on Fig. 3f, g. As we discussed earlier, because of the coherence factors we see only one side of the Fermi pocket. The point at which the dispersing band ends, seemingly abruptly, not only defines the lower edge of the gap but also provides an approximate indication of where the other side of the pocket is located, the two sides of the pocket being approximately symmetric around the turnover point[18,20]. The fact that the turnover points are not centred on the magnetic zone boundary effectively rules out models involving broken symmetries reflecting scattering vectors of the type $\mathbf{Q}(\pi, \pi)$; these result in pockets symmetric around that boundary.

The question then arises as to whether the pairing of electrons above the superconducting transition temperature, T_c, that has been observed in recent experiments[21–23] is also evident in ARPES. Evidence for such phenomena is found in the anti-nodal region (Fig. 4). There the normalized spectra, for temperatures above and below T_c, are shown for two different points on the Fermi surface. The points both show the symmetric gap associated with paired electrons in the superconducting state but differ markedly in the normal state, with the spectrum from point 1 showing asymmetric behaviour and the spectrum from point 2, which is closer to the anti-nodal region, indicating a symmetric gap. The latter apparent symmetry around the Fermi level, similar to that observed in Fig. 1, is a strong indication of the pairing of electrons along the copper–oxygen bond directions in the normal state. Such an observation is consistent with theories that predict the pairing to be essentially one-dimensional in nature[24,25].

Received 5 May; accepted 29 August 2008.

1. Timusk, T. & Statt, B. The pseudogap in high-temperature superconductors: an experimental survey. *Rep. Prog. Phys.* **62**, 61–122 (1999).

2. Valla, T. *et al.* Quasiparticle spectra, charge-density waves, superconductivity, and electron-phonon coupling in 2H-$NbSe_2$. *Phys. Rev. Lett.* **92,** 086401 (2004).
3. Schäfer, J. *et al.* Direct spectroscopic observation of the energy gap formation in the spin density wave phase transition at the Cr(110) surface. *Phys. Rev. Lett.* **83,** 2069–2072 (1999).
4. Chakravarty, S., Laughlin, R. B., Morr, D. K. & Nayak, C. Hidden order in the cuprates. *Phys. Rev. B* **63,** 094503 (2001).
5. Damascelli, A., Hussain, Z. & Shen, Z.-X. Angle-resolved photoemission studies of the cuprate superconductors. *Rev. Mod. Phys.* **75,** 473–541 (2003).
6. Lee, W. S. *et al.* Abrupt onset of a second energy gap at the superconducting transition of underdoped Bi2212. *Nature* **450,** 81–84 (2007).
7. Valla, T., Fedorov, A. V., Lee, J., Davis, J. C. & Gu, G. D. The ground state of the pseudogap in cuprate superconductors. *Science* **314,** 1914–1916 (2006).
8. Tanaka, K. *et al.* Distinct Fermi-momentum-dependent energy gaps in deeply underdoped Bi2212. *Science* **314,** 1910–1913 (2006).
9. Kanigel, A. *et al.* Evolution of the pseudogap from Fermi arcs to the nodal liquid. *Nature Phys.* **2,** 447–451 (2006).
10. Norman, M. R. *et al.* Modeling the Fermi arc in underdoped cuprates. *Phys. Rev. B* **76,** 174501 (2007).
11. Norman, M. R. *et al.* Destruction of the Fermi surface in underdoped high-T_c superconductors. *Nature* **392,** 157–160 (1998).
12. Kisker, E. *et al.* Evidence for the high-spin to low-spin state transition in ordered Fe3Pt Invar. *Phys. Rev. Lett.* **58,** 1784–1787 (1987).
13. Greber, T. *et al.* Photoemission above the Fermi level: the top of the minority *d* band in nickel. *Phys. Rev. Lett.* **79,** 4465–4468 (1997).
14. Matsui, H. *et al.* BCS-like Bogoliubov quasiparticles in high-T_C superconductors observed by angle-resolved photoemission spectroscopy. *Phys. Rev. Lett.* **90,** 217002 (2003).
15. Lucy, L. B. An iterative technique for the rectification of observed distributions. *Astron. J.* **79,** 745–754 (1974).
16. Matsui, H. *et al.* Angle-resolved photoemission spectroscopy of the antiferromagnetic superconductor $Nd_{1.87}Ce_{0.13}CuO_4$: anisotropic spin-correlation gap, pseudogap, and the induced quasiparticle mass enhancement. *Phys. Rev. Lett.* **94,** 047005 (2005).
17. Chakravarty, S. *et al.* Angle-resolved photoemission spectra in the cuprates from the *d*-density wave theory. *Phys. Rev. B* **68,** 100504 (2003).
18. Wen, X. G. & Lee, P. A. Theory of quasiparticles in the underdoped high-T_C superconducting state. *Phys. Rev. Lett.* **80,** 2193–2196 (1998).
19. Konik, R. M., Rice, T. M. & Tsvelik, A. M. Doped spin liquid: Luttinger sum rule and low temperature order. *Phys. Rev. Lett.* **96,** 086407 (2006).
20. Yang, K. Y., Rice, T. M. & Zhang, F. C. Phenomenological theory of the pseudogap state. *Phys. Rev. B* **73,** 174501 (2006).
21. Xu, Z. A. *et al.* Vortex-like excitations and the onset of superconducting phase fluctuation in underdoped $La_{2-x}Sr_xCuO_4$. *Nature* **406,** 486–488 (2000).
22. Wang, Y. *et al.* Field-enhanced diamagnetism in the pseudogap state of the cuprate $Bi_2Sr_2CaCu_2O_{8+d}$ superconductor in an intense magnetic field. *Phys. Rev. Lett.* **95,** 247002 (2005).
23. Wang, Y., Li, L. & Ong, N. P. Nernst effect in high-T_C superconductors. *Phys. Rev. B* **73,** 024510 (2006).
24. Emery, V. J., Kivelson, S. A. & Zachar, O. Spin-gap proximity effect mechanism of high-temperature superconductivity. *Phys. Rev. B* **56,** 6120–6147 (1997).
25. Tsvelik, A. M. & Chubukov, A. V. Phenomenological theory of the underdoped phase of a high-T_c superconductor. *Phys. Rev. Lett.* **98,** 237001 (2007).

Supplementary Information is linked to the online version of the paper at www.nature.com/nature.

Acknowledgements We thank S. Chakravarty, A. Chubukov, P. Lee, M. Norman, M. Rice, D. Scalapino and J. Tranquada for discussions. The assistance of J. Wen and Z. Xu with the preparation of underdoped crystals is also acknowledged. This work was supported by the US Department of Energy.

Author Information Reprints and permissions information is available at www.nature.com/reprints. Correspondence and requests for materials should be addressed to P.D.J. (pdj@bnl.gov).